Dielectric properties of the low dimensional vanadium oxides $Ba_2V_3O_9$ and $Sr_2V_3O_9$

V. Bobnar[a,*,1], P. Lunkenheimer[a], A. Loidl[a], E.E. Kaul[b], C. Geibel[b]

[a]*Experimentalphysik V, Elektronische Korrelationen und Magnetismus, Institut für Physik, Universität Augsburg, D-86135 Augsburg, Germany*
[b]*Max Planck Institut für Chemische Physik fester Stoffe, D-01187 Dresden, Germany*

Ferromagnetism and ferroelectricity are two ordering phenomena which are rather common among transition metal oxides. In contrast, magnetoelectric multiferroics, i.e. compounds which are simultaneously ferroelectric and ferromagnetic (or at least show some kind of magnetic ordering), are rather scarce [1]. They have recently attracted some attention, since one can envisage a whole range of new applications by combining both phenomena. However, in almost all presently known multiferroic compounds, different ions are responsible for the ferroelectric and the magnetic ordering, respectively. Therefore, there seems to be some empirical exclusion principle between both phenomena, but there exists no simple theoretical argument supporting this exclusion. Thus finding new multiferroics where the same ion is responsible for both phenomena would be very stimulating. Exploring the fundamental physics behind the scarcity of multiferroics, it was suggested to look for compounds where a 3d-atom with a partially filled d-shell has an anisotropic coordination providing an asymmetric potential with a double-well potential [1]. In the course of our investigation of low-dimensional ternary vanadium-oxide compounds, we realised that in two compounds, $Sr_2V_3O_9$ and $Ba_2V_3O_9$ the ions reveal such a coordination, and we therefore decided to investigate their dielectric properties.

$Sr_2V_3O_9$ and $Ba_2V_3O_9$ were first synthesised by Bouloux et al. [2]. Despite the identical stoichiometry, they crystallise in different structures [3–6]. Both structures reveal three different V-sites. Two of them show a tetrahedral oxygen-environment and can be assigned to V^{5+}, whereas one site shows an octahedral environment and can be assigned to V^{4+}. The VO_6-octahedra form chains, which are arranged in a different way in the two compounds. In $Sr_2V_3O_9$, the octahedra are linked by common corners, whereas in $Ba_2V_3O_9$ they are linked by common edges. In both compounds, the octahedra are slightly distorted, and the V^{4+}-ion is not located in the centre, but is slightly displaced from the centre by about 25 pm, resulting in the

* Corresponding author. Address: Joz Stefan Institute, P.O. Box 3000, Ljubljana 1001, Slovenia. Tel.: +386-1-4773-763; fax: +386-1-25-19-385.

E-mail address: vid.bobnar@ijs.si (V. Bobnar).

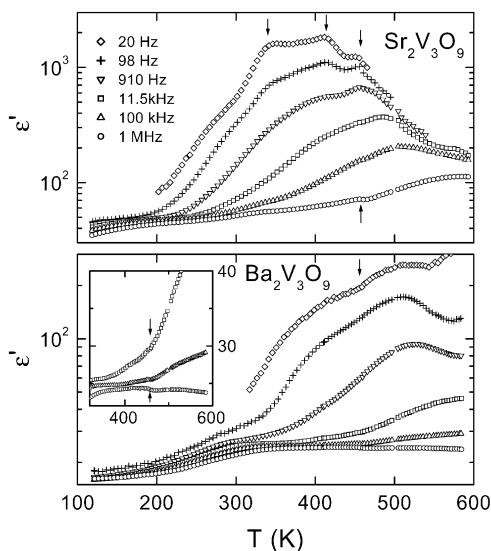[1] On leave from Joz Stefan Institute, Ljubljana, Slovenia.

Fig. 1. Temperature dependence of the dielectric constant of $Sr_2V_3O_9$ and $Ba_2V_3O_9$ for several frequencies. The inset gives a magnified view of the high-temperature/high-frequency region in $Ba_2V_3O_9$. The arrows point out frequency-independent anomalies, indicating possible phase transitions. The curves are shown for temperature ranges only, where the results were within the resolution range of the LCR meter.

formation of one short V–O bond (the Vanadyl-bond), one opposite large V–O bond, and four equatorial bonds of similar, average length towards the O-atoms forming the basal plane. The structural investigations suggest that the V^{4+}-ion might flip from one side of the basal plane to the other, since the refinement of the XR-data [3,5,6] lead to a splitting of the V-site towards both sides of the plane, both sides being statistically occupied. This suggests the existence of a double-well potential, which should be favourable for the formation of a polar ordered state. At the same time, the spin $S = 1/2$ of the V^{4+}-ion provides the magnetism.

Except some preliminary measurements of the magnetic susceptibility [5,6], the physical properties of both compounds have not been investigated so far. No information about the dielectric properties is available. A detailed investigation of the magnetic and thermodynamic properties is currently under way and will be published elsewhere [7]. The results clearly show that both compounds are quasi one-dimensional antiferromagnets with a magnetic exchange $J \approx 90$ K. In the present paper, we present the results of the dielectric measurements.

Single phase polycrystalline samples of $Sr_2V_3O_9$ and $Ba_2V_3O_9$ were synthesised in two steps using a solid state reaction technique. In a first step, we prepared $Sr_2V_2O_7$ and $Ba_2V_2O_7$ by heating a stoichiometric mixture of $SrCO_3$ (respectively, $BaCO_3$) and V_2O_5 in air, first time for 24 h at 850 °C and, after an intermediate grinding, a second time for 24 h at 900 °C. The 239-samples were then prepared by

heating a stoichiometric mixture of 227-powder and VO_2-powder two times (with an intermediate grinding) for 24 h at 900 °C in dynamical high vacuum. This preparation procedure lead to dark-red brown $Sr_2V_3O_9$ and light-red brown $Ba_2V_3O_9$ powder. Neither the crucible material (Al_2O_3 or Pt) nor the form of the starting mixture (intimately mixed powder or pressed pellet) had an influence on the results. The samples were characterised using a STOE powder-diffractometer. For both compounds, the diffracto-grams were fitted using the structure proposed in the literature. No extra peaks corresponding to foreign phases were detected.

For measuring the frequency-dependent complex dielec-tric constant $\varepsilon^* = \varepsilon' - i\varepsilon''$, pressed disc-shaped pellets of the sample material were covered on adjacent faces with silver paint, thereby forming a parallel-plate capacitor. ε^* was measured in the frequency range of 20 Hz–1 MHz using a HP4284A Precision LCR Meter. The amplitude of the probing ac electric signal was 5 V/cm for all measuring frequencies. Using a nitrogen gas heated/cooled cryostat, the data were taken on cooling/heating the system in the temperature range 120 K < T < 600 K with typical rates of ± 0.5 K/min.

In Fig. 1 the temperature dependence of the dielectric constant of both materials investigated is shown for various measurement frequencies. The curves are dominated by a strong step-like increase of $\varepsilon'(T)$ with temperature, shifting towards higher temperatures with increasing frequency, a behaviour very similar to that found for dipolar relaxation processes. Following this increase, for $Sr_2V_3O_9$ and for the lower frequencies in $Ba_2V_3O_9$, a peak in $\varepsilon'(T)$ is observed. Especially for $Sr_2V_3O_9$, where rather high values of $\varepsilon' > 1000$ are reached, the overall behaviour resembles that found in the so-called relaxor-ferroelectric materials [8–10]. However, as will be discussed in detail later, a non-intrinsic origin of the observed huge relaxation steps seems more likely. In addition a second relaxation process of much weaker amplitude shows up in $Ba_2V_3O_9$ at T < 300 K. The onset of similar relaxation steps can be suspected also in $Sr_2V_3O_9$ at T < 200 K.

In addition to those frequency-dependent features, several frequency-independent anomalies in $\varepsilon'(T)$ are observed as indicated by the arrows. Especially for $Sr_2V_3O_9$ for all frequencies investigated an anomaly shows up at 457 K, clearly indicating a phase transition. At about 415 and 340 K additional peaks or shoulders show up, however, at low frequencies only; further investigations are necessary to confirm possible phase transitions at these temperatures. In $Ba_2V_3O_9$ at 456 K a weak anomaly shows up, too, which for the higher frequencies is more clearly seen in the magnified view given in the inset. These anomalies most probably denote structural phase transitions. To check for possible ferroelectricity we measured the dependence of the polarisation P on the ac external electric field E. These experiments were performed at T = 150 K for $Sr_2V_3O_9$ because at higher temperatures the relatively
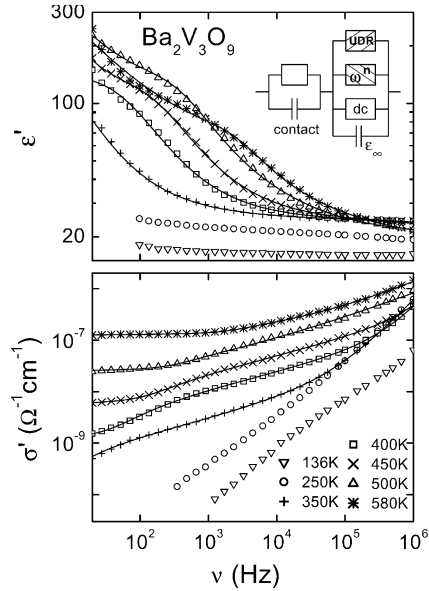
Fig. 2. Frequency dependence of the dielectric constant ε' and conductivity σ', measured at several temperatures in $Ba_2V_3O_9$. Solid lines through the experimental data are fits using the equivalent circuit indicated in the figure.

high conductivity of the sample prevented the determination of the polarisation. Since the conductivity is much lower in $Ba_2V_3O_9$, here the $P(E)$ measurements could be performed at room temperature. For both materials, no non-linearities, i.e. no evidence for polar order was obtained up to external electric fields of 50 kV/cm.

Fig. 2 shows the frequency dependence of the dielectric constant ε' and of the conductivity $\sigma' \sim \varepsilon''\omega$, measured in $Ba_2V_3O_9$ at various temperatures. Several contributions to the dielectric response show up in these spectra. The most pronounced is a distinctive downward step in ε' on increasing frequency. This feature corresponds to the strong relaxation-like feature seen in $\varepsilon'(T)$ (Fig. 1). It is accompanied by a step-like increase in σ' (e.g. from about 6×10^{-9} to 3×10^{-8} Ω^{-1} cm^{-1} for 450 K), which exponentially shifts to higher frequencies with increasing temperature. Such behaviour seems to indicate a dipolar relaxation process with a thermally activated relaxation rate. But also the formation of Schottky diodes at the interface of metal electrodes and semiconducting sample, or internal contacts, i.e. grain boundaries, can drive such a behaviour [11]. At these interfaces depletion layers of low carrier concentration can form, leading to a Maxwell–Wagner type relaxation process. Within this scenario, the frequency-dependent response is described by the equivalent circuit presented in Fig. 2. Solid lines through the experimental data in Fig. 2 are fits using this equivalent circuit, performed simultaneously for ε' and σ'. The agreement is very good, supporting a non-intrinsic origin of the observed strong relaxation features. In the equivalent circuit, the contact

contributions are modelled by a parallel RC circuit [11–15]. At low frequencies the contact contributions dominate the response, leading to the observed, apparently very high values of ε' at low frequencies. At high frequencies the contact capacitance C is effectively shorted, thus allowing the observation of the intrinsic response of the material. At the highest frequencies, ε' saturates at its intrinsic value, decreasing from 24 to 16 with decreasing temperature. For $T > 300$ it is composed of ε_∞, which arises from the ionic and electronic polarisability of the sample, and a contribution from the detected low-temperature relaxation (cf. Fig. 1). At the lowest temperatures, where the relaxation no longer contributes, $\varepsilon_\infty \approx 16$ can be read off. At high frequencies, following the contact steps, the conductivity $\sigma'(\omega)$ seems to approach a plateau, which can be identified with the intrinsic 'bulk' dc conductivity σ_{dc}. However, experimental σ' values still increase. This behaviour can be well described by the so-called universal dielectric response (UDR) with the addition of a dc conductivity [14]

$$\sigma' = \sigma_{dc} + \sigma_0\omega^s, \tag{1}$$

with $s < 1$. The corresponding contribution to the imaginary part [11]

$$\sigma'' = \omega\varepsilon_0\varepsilon' = \tan(s\pi/2)\sigma_0\omega^s, \tag{2}$$

(ε_0 is the permitivity of free space) leads to a smearing out of the Maxwell–Wagner relaxation steps when approaching ε_∞. Several theoretical approaches deduce UDR behaviour from the microscopic transport properties, including hopping over or tunnelling of the charge carriers through an energy barrier separating different localised states [16].

At very low frequencies the dielectric constant is again governed by UDR, leading, e.g. to the additional increase observed at 580 K for $\nu < 300$ Hz (Fig. 2). Namely, the capacitance of the equivalent circuit in the limit $\omega \to 0$ is simply the UDR value, times a factor depending on the intrinsic dc resistivity R_{dc} and resistivity of the contacts R_k: $\varepsilon_0\varepsilon' = \tan(s\pi/2)\sigma_0\omega^{s-1}[R_{dc}/(R_k + R_{dc})]^2$. While usually, even at the lowest frequencies in the experimental frequency window, data are governed only by contact contributions [12–14], in these highly conducting compounds, at higher temperatures the dielectric response is governed again by UDR already below $\nu \approx 100$ Hz.

For $T < 450$ K and at high frequencies, $\sigma'(\omega)$ approaches a power law $\sigma'(\omega) = \sigma_n\omega^n$ with $n \gtrsim 1$, which is not described by the UDR. Thus a further element taking into account this additional super-linear increase was included in the equivalent circuit. As $\varepsilon'' \sim \sigma'/\omega$, an exponent $n > 1$ implies ε'' increasing with frequency. Fig. 3, showing the frequency dependence of ε'' at low temperatures, reveals that in fact $\varepsilon''(\omega)$ exhibits a peak, its low-frequency wing being responsible for the observed super-linear increase in $\sigma'(\omega)$. This loss peak shifts towards lower frequencies for lower temperatures thus indicating the typical slowing down of a dielectric relaxation. The inset of Fig. 3 shows that the relaxation time τ, estimated from the
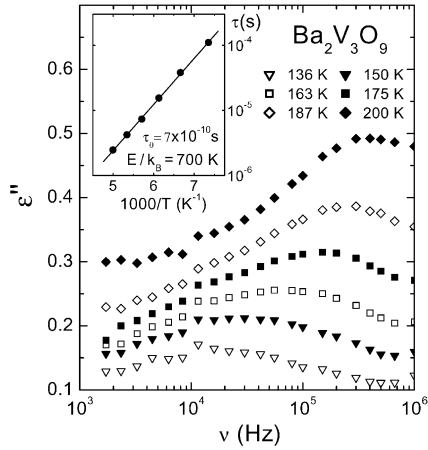
Fig. 3. Frequency dependence of the imaginary part of the complex dielectric constant ε'', measured at several temperatures in the temperature range of $120\,K < T < 200\,K$, indicating a typical slowing down of the dielectric relaxation. The inset shows that the relaxation time τ obeys Arrhenius behaviour with an activation energy of $E/k = 700\,K$.

peak frequency ω_p via $\omega_p\tau = 1$, obeys Arrhenius behaviour $\tau = \tau_0 \exp(E/kT)$ with an activation energy of $E/k_B = 700\,K$. As the temperature decreases, the peaks in ε'' become very broad, revealing that the dielectric mode becomes strongly polydispersive at lower temperatures. At the moment we can only speculate about the microscopic origin of the detected relaxation, but of course it might well be due to the off-centre motion of V^{4+} ions. If our analysis is correct, it means that the V^{4+} ions statistically freeze-in in
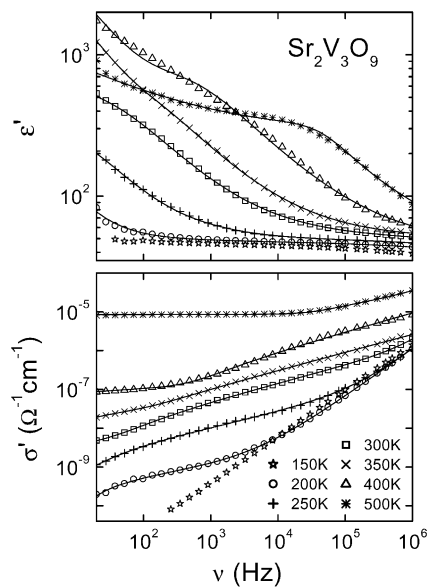

Fig. 4. Frequency dependence of the dielectric constant ε' and conductivity σ', measured at several temperatures in $Sr_2V_3O_9$. Solid lines through the experimental data are fits using the equivalent circuit shown in Fig. 2.

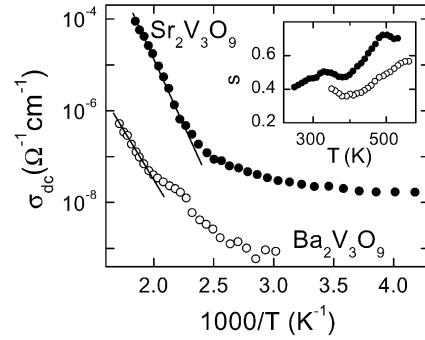Fig. 5. Temperature dependence of the intrinsic dc conductivity ρ_{dc}, determined from fits, in $Ba_2V_3O_9$ and in $Sr_2V_3O_9$ (Arrhenius representation). The inset shows the temperature dependence of the UDR parameter s in both compounds.

their off-centre positions and do not reach long-range structural order.

Similar results as in $Ba_2V_3O_9$ were also obtained in $Sr_2V_3O_9$. Fig. 4 shows the frequency dependence of the dielectric constant ε' and conductivity σ', measured in $Sr_2V_3O_9$ at several temperatures. All contributions to the dielectric response, already mentioned earlier, were also detected in this compound. Thus solid lines through the experimental data present fits using the same equivalent circuit, shown already in Fig. 2. As noted already in the discussion of Fig. 1, a low-temperature relaxation is also present in $Sr_2V_3O_9$. It leads to a super-linear increase of $\sigma'(\omega)$, e.g. observed very clearly at 150 K. However, the characteristic time of this relaxation is shifted towards too high frequencies to permit a detailed evaluation. As can be read off at the lowest temperatures, the intrinsic ε', composed of ε_∞ and the contribution from the low-temperature relaxation, amounts about 50.

Fig. 5 shows the temperature dependence of the intrinsic dc conductivity ρ_{dc}, determined from the fits in both compounds. As expected, concerning the fact that the measured conductivity σ' was always lower in $Ba_2V_3O_9$ than in $Sr_2V_3O_9$, the intrinsic σ_{dc} values are much lower in $Ba_2V_3O_9$. In both compounds, at high-temperatures $\rho_{dc}(\omega)$ can be described by Arrhenius behaviour with energy barriers of 0.86 eV for $Ba_2V_3O_9$ and 1.1 eV for $Sr_2V_3O_9$. However, at $T < 500\,K$ for $Ba_2V_3O_9$ and at $T < 440\,K$ for $Sr_2V_3O_9$ deviations show up that may indicate a transition to non-thermally activated hopping of localised charge carriers as the dominant charge transport mechanism at lower temperatures. The inset shows the temperature dependence of the parameter s of UDR in both compounds. This dependence should, in principle, reveal details on the mechanism of hopping (e.g. small-polaron tunnelling, thermally activated hopping, etc.) [16]. However, because ε_∞ and the low-temperature relaxation dominate the response at low temperatures in both compounds, measurements in a much broader frequency interval are necessary in order to determine values of s also at lower temperatures,

which is prerequisite for an unequivocal determination of the hopping mechanism.

In conclusion, we have investigated the dielectric response of the low dimensional vanadium oxides $Ba_2V_3O_9$ and $Sr_2V_3O_9$ in the frequency range of 20 Hz– 1 MHz. From frequency-independent anomalies in $\varepsilon(\omega)$ evidence for a (most probably structural) phase transition close to 455 K in both materials can be deduced. In addition in $Sr_2V_3O_9$ there are indications for two further transitions at 415 and 340 K. For both materials, the low-frequency response is dominated by a strong relaxation-like feature. While we cannot fully exclude an intrinsic origin of this behaviour, it seems very likely that the response in this region is governed by non-intrinsic contact contributions. This notion is supported by an analysis of the spectra in terms of an equivalent circuit, revealing the intrinsic dielectric constants and dc conductivities of these systems. In addition, we found evidence for UDR behaviour, characteristic for hopping of localised charge carriers, and detected a dielectric relaxation process at low temperatures in both materials. Although in both compounds the coordination of the V^{4+}-ion was thought to be favourable for the occurrence of (anti-)ferroelectricity, we did not find evidence for such a transition, but we only observed a slightly enhanced dielectric constant. This result is therefore a further confirmation of the empirical exclusion principle between ferromagnetism and ferroelectricity.

References

[1] N.A. Hill, J. Phys. Chem. B 104 (2000) 6694.
[2] J.C. Bouloux, J. Galy, P. Hagenmüller, Rev. Chim. Miner. 11 (1974) 48.
[3] J. Feldmann, H. Müller-Buschbaum, Z. Naturforsch. 50b (1995) 43.
[4] J. Feldmann, H. Müller-Buschbaum, Z. Naturforsch. 51b (1996) 489.
[5] O. Mentre, A.C. Dhaussy, F. Abraham, H. Steinfink, J. Solid State Chem. 140 (1998) 417.
[6] A.C. Dhaussy, F. Abraham, O. Mentre, H. Steinfink, J. Solid State Chem. 126 (1996) 328.
[7] E.E. Kaul et al., to be published.
[8] G.A. Smolenskii, J. Phys. Soc. Jpn 28 (1970) 26.
[9] L.E. Cross, Ferroelectrics 76 (1987) 241.
[10] N. Setter, L.E. Cross, J. Appl. Phys. 51 (1980) 4356.
[11] A.K. Jonscher, Dielectric Relaxations in Solids, Chelsea Dielectrics Press, London, 1983.
[12] P. Lunkenheimer, M. Resch, A. Loidl, Y. Hidaka, Phys. Rev. Lett. 69 (1992) 498.
[13] P. Lunkenheimer, G. Knebel, A. Pimenov, G.A. Emelchenko, A. Loidl, Z. Phys. B 99 (1996) 507.
[14] A. Seeger, P. Lunkenheimer, J. Hemberger, A.A. Mukhin, V.Yu. Ivanov, A.M. Balbashov, A. Loidl, J. Phys.: Condens. Matter 11 (1999) 3273.
[15] P. Lunkenheimer, V. Bobnar, A.V. Pronin, A.I. Ritus, A.A. Volkov, A. Loidl, cond-mat/0201146.
[16] S.R. Elliott, Adv. Phys. 36 (1987) 135.